Multiscale assessment of the accuracy of surface replication

Julie Marteau, M Wieczorowski, Y Xia, Maxence Bigerelle

Multiscale assessment of the accuracy of surface replication

J Marteau[1], M Wieczorowski[2], Y Xia[3] and M Bigerelle[1]

[1] LAMIH, UMR-CNRS 8201, Bâtiment CISIT, Université de Valenciennes et du Hainaut-Cambrésis, Le Mont Houy, F59313 Valenciennes CEDEX 9, France
[2] Poznan University of Technology, Faculty of Mechanical Engineering and Management, Institute of Mechanical Technology, Piotrowo 3, 60-965 Poznan, Poland
[3] Laboratoire Roberval, UMR-CNRS 7337, Université de Technologie de Compiègne, Centre de Recherches de Royallieu, CS 60319, 60203 Compiègne Cedex, France

E-mail: julie.marteau1@gmail.com

Abstract

This paper presents a methodology for the assessment of replication accuracy using a multiscale approach. It focuses on the quantification of 'metrological replication accuracy', which is a direct comparison of the topography of a surface and its replica. This methodology uses an analysis of variance and takes into account the variability of the experimental results. To assess replication accuracy, the differences in either one or several roughness parameter values of a surface and its replica are assessed over different scales, using the F-value as an indicator. In order to get a multiscale comparison, the surfaces are examined using 17 cut-off lengths with three types of filters (high-pass, low-pass and band-pass). This methodology enables us to identify the scales at which the topography features are best replicated. Transfer functions of roughness parameters are also observed to quantify the differences between the studied surface and its replica. This methodology is applied to the study of the replication of ground titanium alloy specimens having rough to mirror-like surfaces. It enables us to show that the studied replica material enables the accurate reproduction of rough surfaces but gives inaccurate results for the replication of smooth surfaces.

Keywords: replication, topography, multiscale, roughness

1. Introduction

To be able to measure inaccessible mechanical components such as the interior surface of Nb superconducting radio-frequency accelerator cavities [1] and aircraft engines [2], surface replication is a widely used tool. It is also frequently used in order to characterize body parts [3], skin [4, 5], or components that are either too large (e.g. foils [6], rock fracture [7]) or too heavy to be directly measured, or else that simply cannot be measured without dismantling an entire system. Motivations for using replica techniques for surface characterization also arise from the fact that they enable the creation of biocompatible surfaces (e.g. [8]). The use of replication also enables one to keep a record of surface changes. Replicas can be used as a kind of data storage when studying phenomena such as wear [9–12], crack detection [13, 14], skin diseases or aging [15, 16]. Finally, replication is also used to explore the manufacturing of biomimetic surfaces [17, 18].

However, in any replication, there is loss of information. Replicas are not a perfect negative image of the parent surface. Their quality depends on the replica material, the topography and the process conditions (e.g. gas bubbles forming pores). Several types of materials were developed for the replication of surface features from the macroscale to the nanoscale. Liu *et al* [19] studied the accuracy of three different replica materials (Repliset, Technovit and Press-O-Film) by replicating four engineering ground surfaces with average roughness values ranging from 0.2 μm to 1.6 μm. To assess replica accuracy, they used the same locations for the measurement of profiles on the replicas and the original surfaces. They qualitatively compared the replicas and the original surfaces and then used the arithmetic mean roughness R_a using cut-off lengths equal to 0.2, 0.4, 0.8 and 1.6 μm. The

use of this roughness parameter gives a good general description of height variations but remains insufficient to describe the peaks and valleys in detail. Nilsson *et al* [20] tested three different replica materials (Araldite, Microset and Technovit) on five types of machined surfaces varying from smooth to rough and covering stochastic as well as deterministic surfaces (shot-blasted texturing, electron beam texturing, surface grinding, crankshaft and cylinder liner). Similarly to Liu *et al* [19], Nilsson *et al* [20] scanned areas having the same locations on the replica and the original surface but they used five three-dimensional (3D) surface parameters to assess the accuracy of the replicas: S_a, S_z, S_m, S_c and S_z. Balcon *et al* [21] discussed different ways to analyze the accuracy of surface replication. First, they emphasized the need to think of the analysis in terms of functionality relevance for the work piece. Then, using simulated surfaces and replicas, they assessed the information given by roughness parameters (areal and volume related parameters), cross-correlation indices (a measure of the similarity between two surfaces) and Fourier-related parameters (periodic distributions and surface orientation). These few examples show the main strategies used to characterize replication accuracy. As underlined by Hansen *et al* [22], the authors generally define the degree of replication related to their specific investigations. This point should be clarified. There are three ways to determine replication quality, depending on the analysis purpose:

(i) 'Quantification of metrological replication accuracy': direct comparison of the topography of a given surface and its replica.
(ii) 'Quantification of physical replication accuracy': the examined surfaces show different topographies caused by the evolution of some physical phenomenon. An answer to the following question is sought: Do the replicas enable us to find a relation between the physical phenomenon that created the surface topography and the differences of roughness?
(iii) 'Quantification of functionality replication accuracy': the examined series of surfaces is linked to some physical phenomenon or functionality. A link is searched between the replicas and the functionality of the original surfaces, without taking into account the surface topography of the original surface.

The aim of this article is to present a methodology enabling us to quantify metrological replication accuracy. It is designed to assess the quality of replicas calculating approximately 50 types of roughness parameters over different scales (17 cut-off lengths and three filter types).

2. Materials and methods

2.1. Original specimens

The original surfaces are titanium alloy (TiAl6V4) specimens abraded with different silicon carbide grit-papers ranging from 80 (rough surfaces) to 2400 (near mirror-like surfaces). These grit sizes correspond to the size of the particles embedded in the sandpaper, established by the European Federation of European Producers of Abrasives (P grade). 80 grit paper means that the particle average diameter is equal to 201 μm. The particle average diameter of 2400 grit paper is approximately equal to 8 μm.

Seven samples were first cut from a 30 mm diameter bar into 20 mm thick discs. Then, they were all polished to 4000 grit paper with an automatic grinding machine in order to get similar initial states. Next, several types of topography were achieved by using different grit papers under identical force and time conditions (150 N, 3 min) with water lubrication. The different surfaces are hereafter named using the number of the last abrasive grading scale of sandpaper i.e. 80, 120, 220, 500, 800, 1200 and 2400.

2.2. Replica material

The material used for the replicas is MD-3P from Plastiform® (France). It is made of three components (resin, powder and hardening agent), which polymerize at room temperature after mixing. The mixture is opaque and has a liquid initial consistency. After a curing time of 10 min, rigid impressions are obtained.

2.3. Roughness measurements

The original surfaces and the replicas were measured using a 3D non-contact optical profilometer (Zygo NewView™ 7300, Zygo Corp., USA) with a ×20 objective lens. The lateral resolution is equal to 760 nm and the vertical resolution is about 3 nm. In order to study large areas without deteriorating the field of view, the stitching function was used. The dimensions of the stitched surfaces are 1189 μm × 891 μm having 2176 × 1632 points. Each surface was rectified using a polynomial of degree 3.

2.4. Multiscale roughness characterization

Typically, surface topography is quickly analyzed using the arithmetic mean deviation S_a. Other amplitude parameters are sometimes used, such as the root-mean-square deviation of the surface S_q or the maximum height of the surface S_z. In the following characterization, 49 roughness parameters [23–25] were calculated in order to assess the quality of the replicas. There were amplitude parameters, but also hybrid parameters such as the density of summits S_{ds}, functional volume parameters such as the void volume V_v or the material volume $V_{m,}$ or functional parameters such as the reduced peak height S_{pk} or the kernel roughness depth S_k. All these parameters were evaluated using 17 cut-off lengths (equal to 6, 9, 10, 13, 15, 19, 23, 29, 36, 45, 56, 74, 99, 127, 178, 297 and 446 μm) with three types of Robust Gaussian filters [26] (high pass, low pass and band-pass) in order to get a multiscale roughness characterization. For the band-pass filter, each indicated value corresponds to the lower cut-off length, while the bandwidth is equal to the following greater value subtracted by the lower cut-off length. For example, when the cut-off length is equal to 99 μm then the bandwidth is equal to $127 - 99 = 28$ μm. The intervals between each cut-off length were chosen in order to get a resolution equal to the one of the bandwidth.

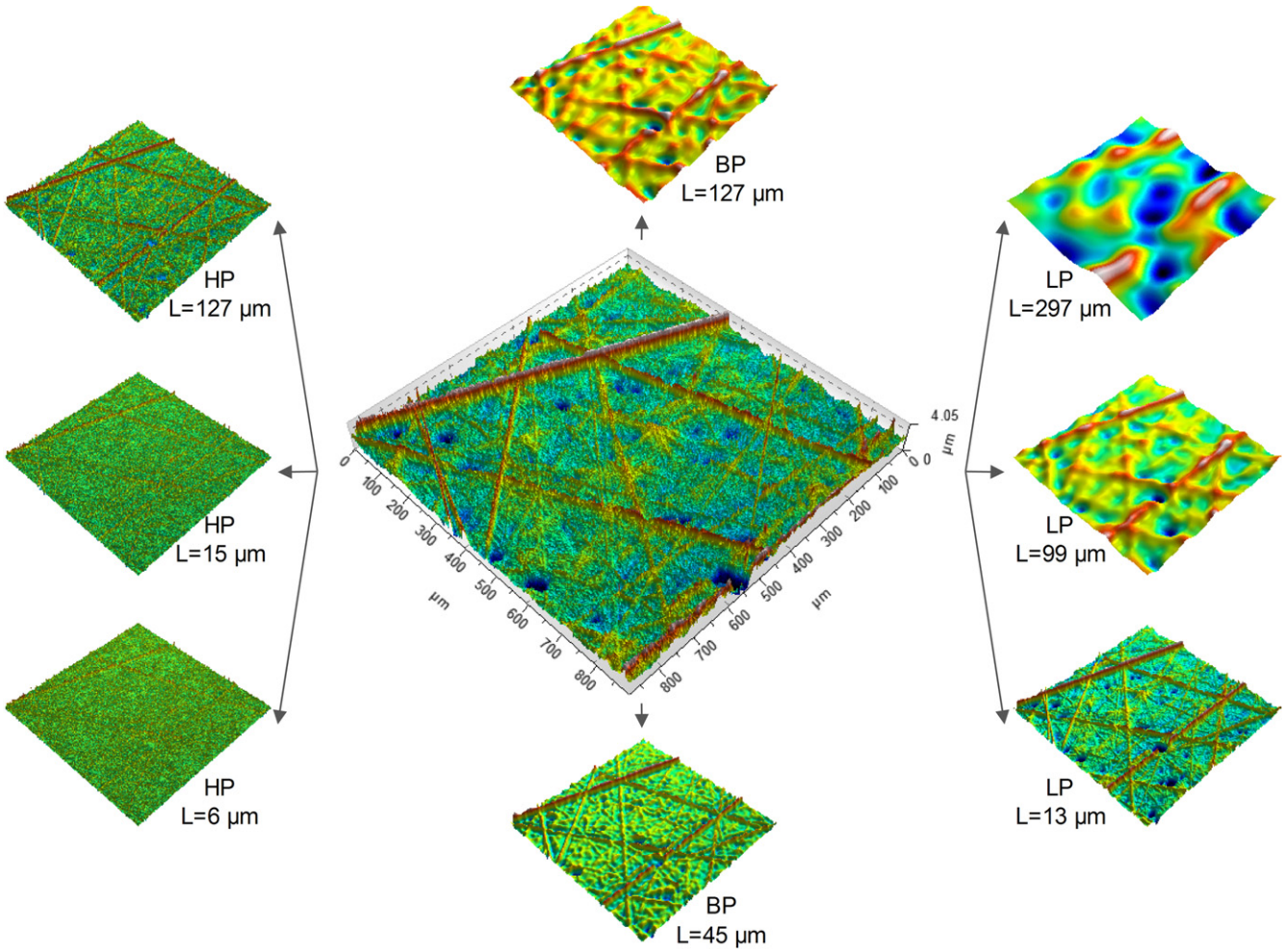

Figure 1. Example of measurement of the specimen polished with 120 grit paper and the surfaces obtained using different types of filtering: a high-pass filter (HP) with cut-off lengths equal to 6, 15 and 127 μm; a low-pass filter (LP) with cut-off lengths equal to 13, 99 and 297 μm; and a band-pass filter (BP) with cut-off lengths equal to 45 and 127 μm (with bandwidths equal to 11 and 51 μm, respectively).

This choice enables us to decrease the number of analyzed cut-off filters. Figure 1 shows one of the measurements of the specimen polished with 120 grit paper and the surfaces obtained using different kinds of filtering: a band-pass filter with cut-off lengths equal to 45 and 127 μm (with bandwidths equal to 11 and 51 μm, respectively); a high-pass filter with cut-off lengths equal to 6, 15 and 127 μm; and a low-pass filter with cut-off lengths equal to 13, 99 and 297 μm. This figure shows that very different surface features are highlighted depending on the filtering.

Similarly, depending on the cut-off value, substantially different results are obtained for the roughness parameters. Figure 2 shows the variation of the arithmetic mean deviation S_a values with the use of different filters and cut-off lengths, for the replica of the specimen polished with 80 grit paper. The confidence intervals of figure 2 represent the variations of mean obtained with the bootstrap technique, thoroughly described in the following section. The use of a high-pass filter leads to an increase of S_a with an increase of the cut-off length. This increase of roughness amplitude reflects a fractal trend: as the cut-off length increases, more and more topography details are observed. In fact, many engineering

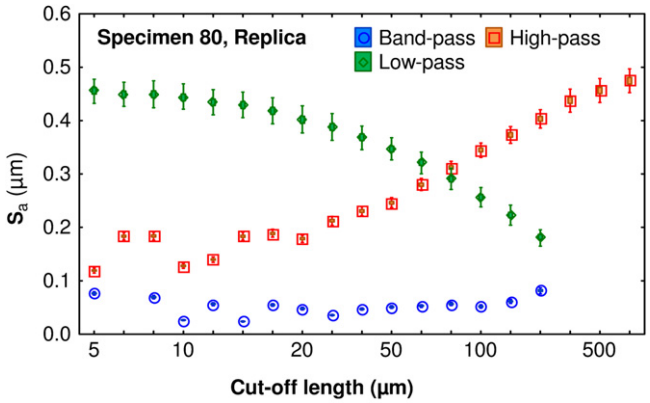

Figure 2. Arithmetic mean deviation S_a versus cut-off lengths for the replica of the specimen polished with 80 grit paper using low-pass, high-pass and band-pass filters.

surfaces are fractal [27]. The authors [28, 29] showed that ground surfaces are fractal. If the examined surfaces are self-affine fractal, then they have a $1/f^{\alpha}$ spectrum (Hooge's law of $1/F$ noise [30]). It means that the decrease of the spectrum amplitude component follows a power law [31]. The arithmetic

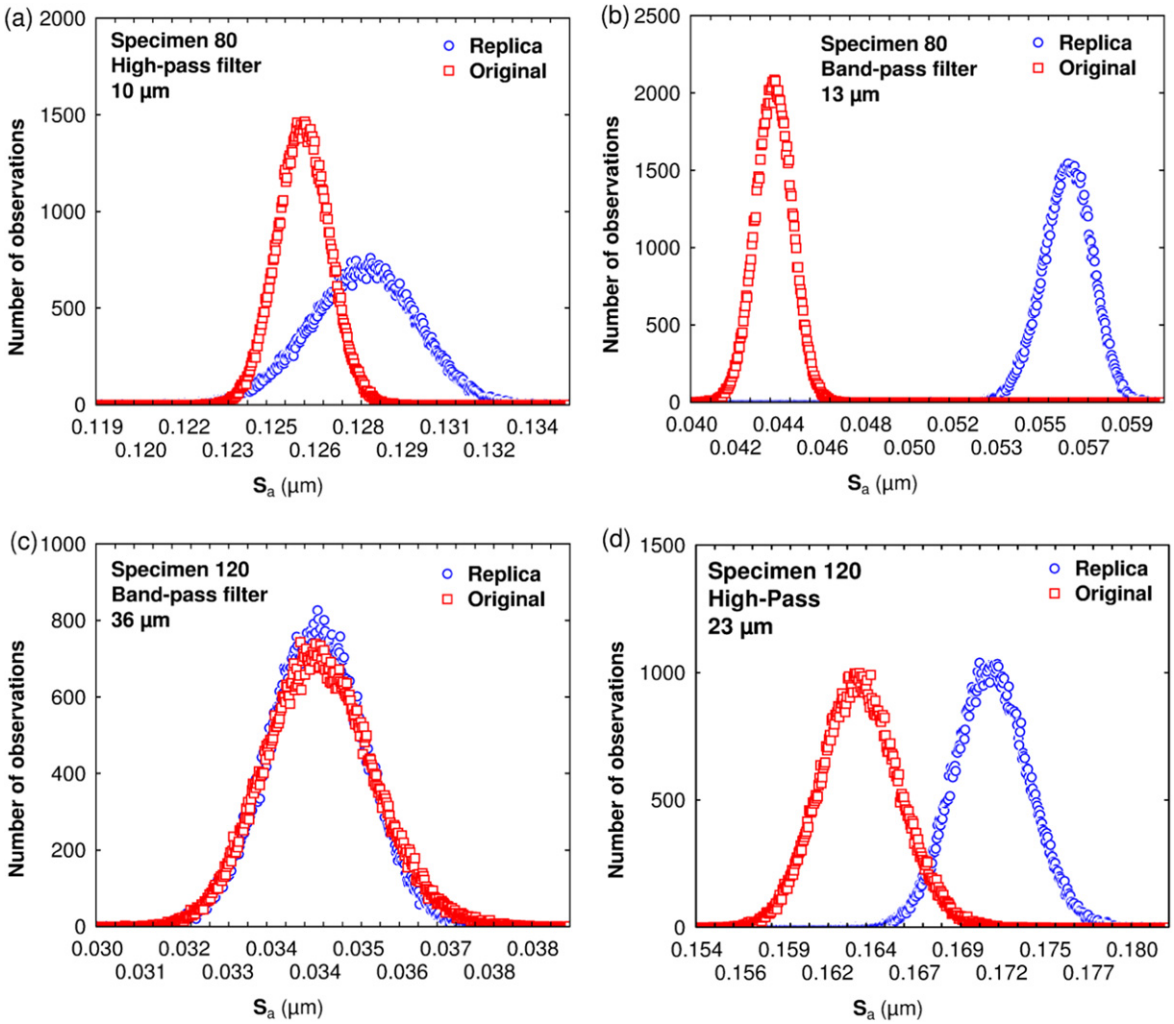

Figure 3. Bootstrapped probability density function of the mean of S_a values of (a) the original surface polished with 80 grit paper and its replica using a high-pass filter and a cut-off length equal to 10 μm, (b) the original surface polished with 80 grit paper and its replica using a band-pass filter and a cut-off length equal to 13 μm, (c) the original surface polished with 120 grit paper and its replica using a band-pass filter and a cut-off length equal to 36 μm, and (d) the original surface polished with 120 grit paper and its replica using a high-pass filter and a cut-off length equal to 23 μm.

mean deviation S_a follows it too, under some conditions [32], even if the surfaces are anisotropic [33]. The use of low-pass filtering induces a surface defractalization: there are fewer details with the use of larger cut-off lengths. For small cut-off lengths, the removal of roughness created by small wavelengths has little effect on roughness amplitude (fractal dimension). However, when the cut-off length becomes larger than the surface auto-correlation length, there is a clear drop of the amplitude of the small frequencies. For the band-pass filter, the results are more difficult to interpret. The arithmetic mean deviation seems almost constant along the longitudinal axis. However, the bandwidth varies with the indicated cut-off values as it follows a power law. Besides, the impulse response of the filter probably contributes to this effect.

2.5. Quantitative assessment of replication accuracy

Replication accuracy is assessed using an analysis of variance (ANOVA) with a recent resampling technique called bootstrap [34]. An algorithm was developed by the authors using the capabilities of the SAS (statistical analysis system) language to quantitatively determine the degree of resemblance of the replicas and original surfaces. For this purpose, for each roughness parameter computed with a given cut-off length and filter type, the F-statistic is calculated using one class: the surface type. The latter has two levels: the original surface and the replica. It is worth noting that a student test could have been used instead of a Fisher test. Indeed, those tests are perfectly equivalent when only one class is observed. However, due to previous and future developments requiring more than one class, the Fisher-test was preferred.

The F-index value enables us to rank the degree of resemblance. If F is close to 1, then replication does not change the filtered topography computed with the tested roughness parameter. Conversely, the higher the value of F, the higher the differences of results between the replica and the original surface are for the studied roughness parameter and filtering conditions.

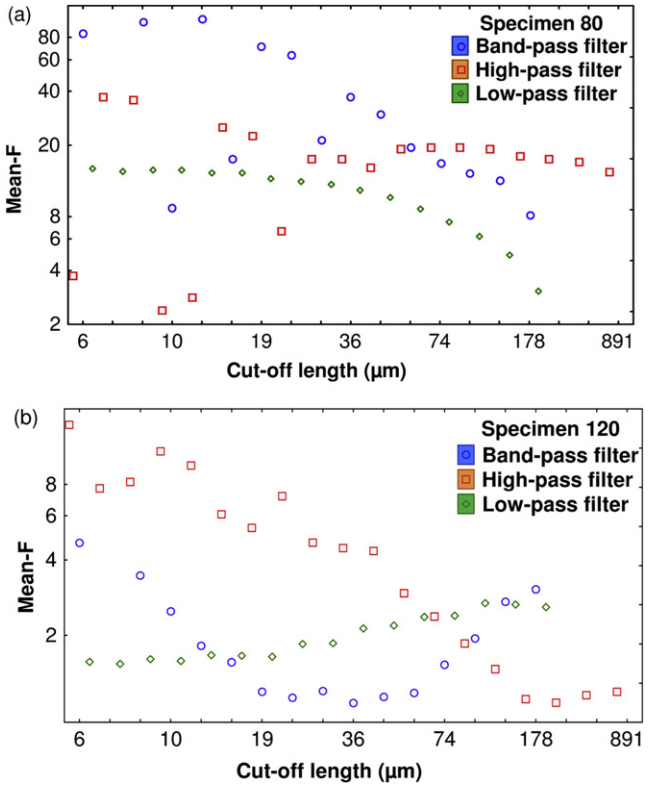

Figure 4. Mean of the F-statistic given by the comparison of the arithmetic mean deviation S_a of the replica and the original surface of TiAl6V4 polished with (a) 80 grit paper (b) 120 grit paper as a function of cut-off lengths, using a low-pass filter, high pass filter and band-pass filter.

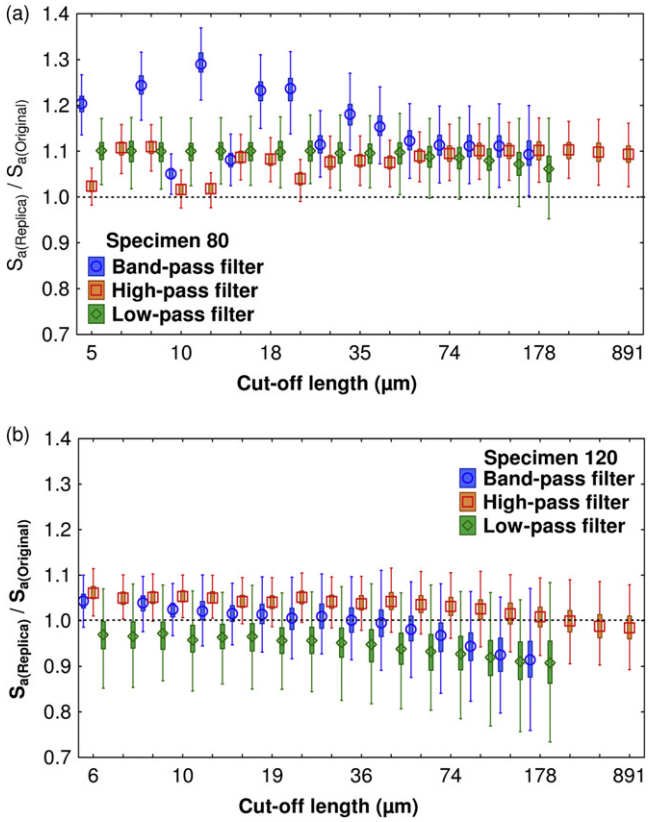

Figure 5. Transfer function of the arithmetic mean deviation S_a versus cut-off lengths using low-pass, high-pass and band-pass filters, for the specimens polished with (a) 80 grit paper and (b) 120 grit paper.

Small disturbances in the experimental data set are known to influence the ANOVA results. Thus, the variability of F is taken into account using the bootstrap method. The latter consists in generating a large number N of simulated bootstrap samples ($N = 500$ in this study) from an experimental data set of size K ($K = 20$ roughness measurements). A bootstrap sample is obtained by randomly sampling with replacement experimental data scores. Each score has a probability equal to $1/K$ to be selected. A bootstrap sample is thus not identical to the original experimental set as it contains a new selection of scores (some values of the experimental set may appear once or twice whereas others may not appear).

3. Illustration of the proposed methodology with the arithmetic mean deviation S_a

To begin with, the proposed methodology is described using a single parameter: the arithmetic mean deviation S_a. This parameter was chosen because it remains the most used parameter when analyzing roughness. After illustrating the proposed methodology with this roughness parameter, it will be applied to all the roughness parameters.

In order to assess replication accuracy, the differences of S_a values between the replica and the original surface must be gauged. As previously stated, surfaces cannot be perfectly replicated: there is always loss of information. Replication may be successful for some features of the surface but not for others i.e. the microroughness may be well reproduced, while the waviness of the original surface may not be correctly duplicated. To fully assess replication accuracy, a multiscale study of roughness is required. It is done through the use of three types of Robut Gaussian filters (low pass, high pass and band-pass) and 17 cut-off lengths for the calculation of the arithmetic mean deviation. Figure 3 shows intermediate and extreme results obtained for Specimen 80 and 120: it depicts the bootstrapped probability density function of the mean of S_a of both the original surfaces and corresponding replicas. It can be seen that significantly different results are obtained depending on the filtering conditions (i.e. the choice of filter and cut-off length) and the examined topography. The bootstrap enables us to observe the spread around the mean of the S_a values and thus to assess whether the differences of S_a values are significant. The bootstrapped probability density function of the mean of S_a of both the original surface polished with 120 grit paper and its replica computed using a band-pass filter with a cut-off length equal to 36 μm [figure 3(c)] overlap. Thus, it can be concluded that the mean S_a is similar for this filter, at the examined scale. Conversely, figure 3(b) shows that the means of S_a are significantly different for Specimen 80 when calculating this roughness parameter with a band-pass filter and a cut-off equal to 13 μm. Figures 3(a) and (c) show intermediate results: the

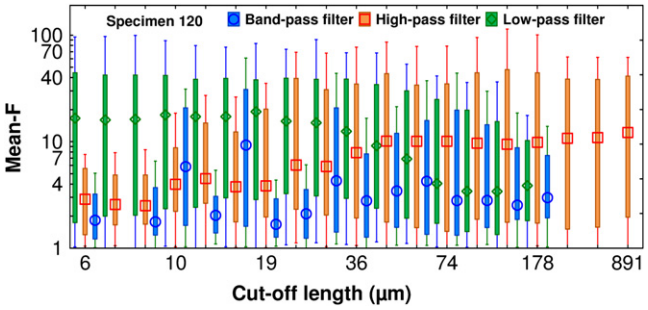

Figure 6. Mean of the F-statistic obtained when comparing the results of 49 roughness parameters to assess the differences between the surface of TiAl6V4 polished with 120 grit paper and its replica versus cut-off length using low-pass, high-pass and band-pass filters.

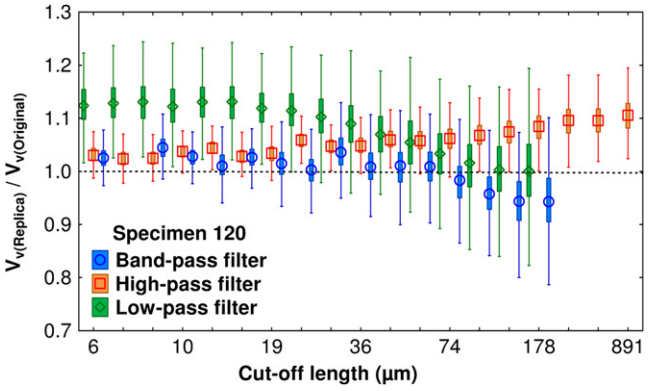

Figure 7. Transfer function of the void volume V_v for a material ratio equal to 10% versus cut-off lengths using low-pass, high-pass and band-pass filters.

bootstrapped probability density function of the mean of S_a of both the original surfaces and corresponding replicas overlap, even if not perfectly.

These differences of mean S_a values show that there are differences of topography between the original surface and its replica. These differences could be quantified by computing the area of the probability density functions. However, the F-values represent a more straightforward means of comparison of the mean S_a values of the original surface and its replica. Figure 4 shows the mean of F obtained for the replicas and original surfaces polished with (a) 80 grit paper and (b) 120 grit paper as a function of cut-off lengths using low pass, high pass and band-pass filters. If F is near to unity, then the differences between the arithmetic mean deviation S_a of the original surface and the one of the replica cannot be seen as significant. The larger the number F, the greater the difference between the S_a values of the original surface and its replica. Figure 4(a) shows F-values ranging from 2 to 100 while figure 4(b) shows values ranging from 1 to 14. Thus, the S_a values of the original surface polished with 80 grit paper and its replica are globally more significantly different than the ones of Specimen 120 and its replica. Specimen 120 was thus better replicated than Specimen 80 according to this roughness parameter.

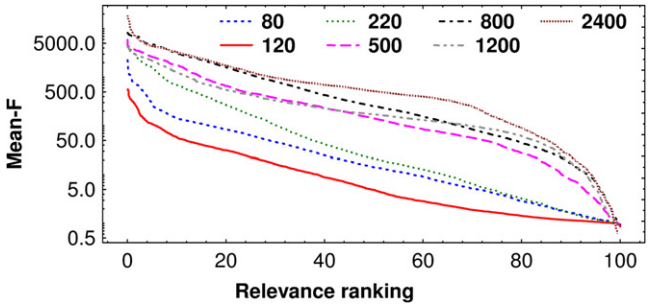

Figure 8. Mean of F versus relevance ranking for the specimens polished with grit-paper 80, 120, 220, 500, 800, 1200 and 2400.

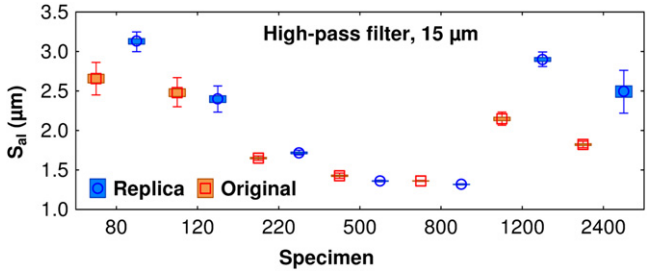

Figure 9. Mean of the fastest decay autocorrelation rate S_{al} of the original surfaces and their replicas as a function of the specimen numbers, calculated using a high-pass filter with a cut-off length equal to 15 μm.

A quick comparison of the two specimens, using figure 4 also reveals that they show different trends. For instance, Specimen 80 shows constant F-mean values approximately equal to 15 for cut-off lengths ranging from 6 to 36 μm and then F-mean decreases from 15 to 4 for cut-off lengths larger than 36 μm. Conversely, Specimen 120 shows constant F-mean values approximately equal to 1 for cut-off lengths ranging from 6 to 19 μm, and then the F-mean slightly increases from 1 to 3 for cut-off lengths larger than 19 μm. Different variations are also found for the high-pass and band-pass filters. Finding F-mean values larger than 1 for both specimens whatever the cut-off length and the type of filter means that the waviness (global shapes) and the micro-roughness (small details) show different mean S_a value. It implies that the replication does not enable us to accurately reproduce the topography amplitude of the specimens, whatever the studied scale.

F-mean is a good indicator to assess the quality of replication of roughness and waviness at different scales; it enables us to indicate which topographical features are best reproduced. However, it does not give details about the topographical changes. For example, the value of F-mean does not enable us to measure if the replica microroughness is higher or lower than the one of the original surface. Another indicator may then be used: the transfer function of the examined roughness parameter. Figure 5 shows the results found for the function transfer of S_a ($S_{a\ (replica)}/S_{a\ (original)}$) of the replication of the surface polished with (a) 80 grit paper and (b) 120 grit paper as a function of cut-off lengths for three

types of filter. For Specimen 80, the transfer function values are globally larger than unity, whatever the filter type and cut-off length values. Thus, the replica has larger S_a values than the original surface over all the scales. For Specimen 120, the transfer function values are approximately equal to 1 for the low-pass and band-pass filters. The bootstrapped values show a large variability, particularly when using a low-pass filter or a band-pass filter with cut-off lengths larger than 45 μm. The transfer function values are significantly larger than one and show less variability when using a high-pass filter with low cut-off lengths. It thus seems that the replica microroughness is larger than the original microroughness.

This first application of the methodology to the arithmetic mean deviation S_a enabled us to emphasize its relevance and efficiency for the assessment of replication accuracy. In the following section, the proposed methodology is simultaneously applied to 49 roughness parameters.

4. Application of the proposed methodology to all the calculated roughness parameters

In this section, the differences between the original surfaces and their replica are assessed by simultaneously using 49 roughness parameters instead of only observing the variation of the arithmetic mean deviation S_a parameter. Thus, the F-statistic now describes the differences observed in all the parameters, between the original surface and its replica. Figure 6 shows the mean of F as a function of cut-off lengths for low pass, high pass and band-pass filters, for Specimen 120. The best results over the range of cut-off lengths (i.e. the lowest F values) are found using the band-pass filter. For the low-pass filter, the mean of F is between 15 and 20 for cut-off lengths lower than 29 μm. The best results for this filter are obtained for large cut-off lengths. On the contrary, for the high pass filter, the best results are obtained for small cut-off lengths. Figure 6 gives an overview of the replication accuracy and enables to assess replication accuracy by simultaneously comparing several roughness parameters. It should be noted that any combination of roughness parameters could be used. For example, one may need to check if heights and spacing of motifs are well replicated. In this case, the F-mean corresponding to the needed roughness parameters could be calculated and examined.

Transfer functions of particular roughness parameters should be observed to better understand the differences of topography between the original surface and its replica. For example, figure 7 shows the transfer function of the void volume at a material ratio equal to 10%. With the low pass filter and high pass filter, the void volume of the replica is always larger than the one of the original surface. Thus, it means that the replica lacks details.

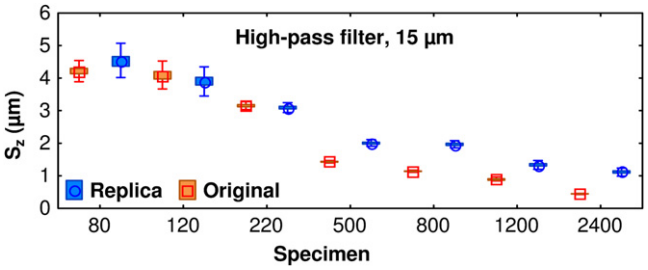

Figure 10. Mean of the maximum height of the surface S_z of the original surfaces and their replicas as a function of the specimen numbers, calculated using a high-pass filter with a cut-off length equal to 15 μm.

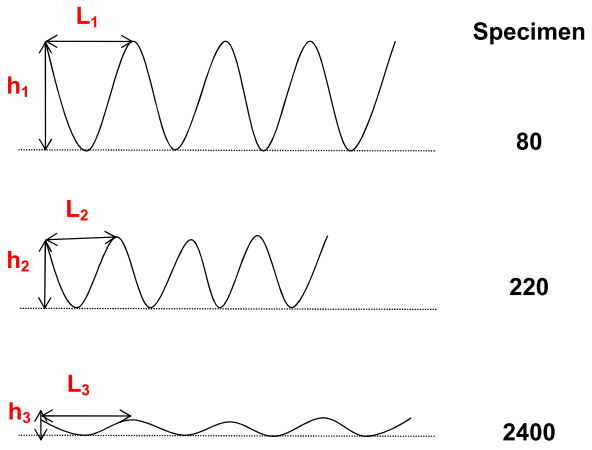

Figure 11. Diagram of the roughness of the specimens polished with 80 grit, 220 grit and 2400 grit papers.

For the sake of brevity, the methodology was presented using only the results of the specimen polished with 120 grit paper and its replica. However, all the analyses were conducted on the seven polished specimens (80, 120, 220, 500, 800, 1200 and 2400) and their corresponding replicas. Figure 8 shows the mean of F of all the specimens as a function of the relevance ranking. The latter is only used to view the mean of F of all the specimens on the same scale, from the largest to the lowest value. Figure 8 shows that the best results for the replication are obtained for Specimen 120. Indeed, the lowest values are obtained for the mean of F, which means that fewer differences are observed between the 49 roughness parameters of the original surface and its replica. On the contrary, Specimen 2400 and 800 show the greatest number of differences as the values of the mean of F are particularly high.

Table 1. Values of the indicator of defaults Deft for the replication of the specimens polished with paper grit 80, 120, 220, 500, 800, 1200 and 2400.

Specimen	80	120	220	500	800	1200	2400
Deft	0.85	0.73	0.86	0.96	0.97	0.96	0.97

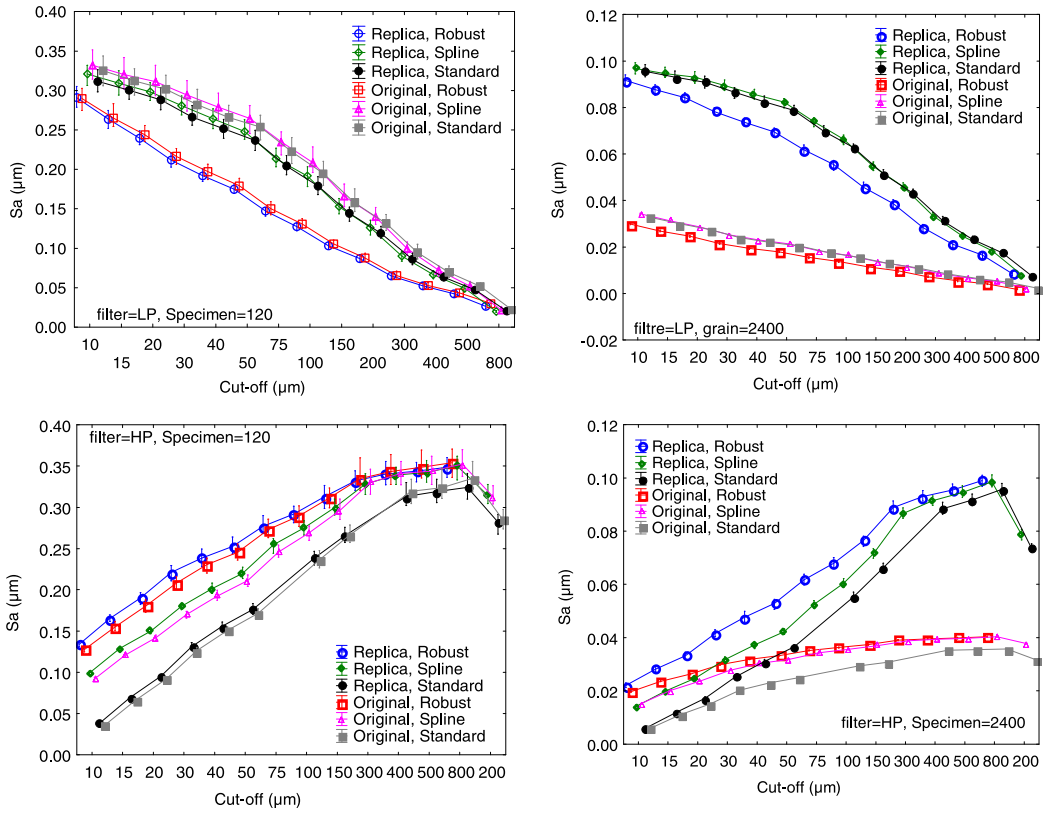

Figure A1. Arithmetic mean deviation S_a as a function of the cut-off length, for the original surfaces polished with 120 and 2400 grit paper and their respective replicas, calculated using high-pass and low-pass Gaussian filters, Robust filters and Spline filters.

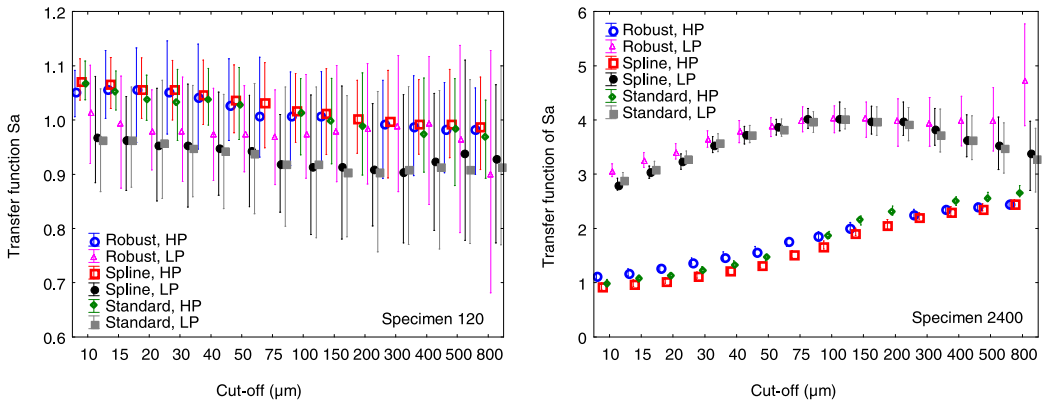

Figure A2. Transfer function of the arithmetic mean deviation S_a as a function of the cut-off length, for the original surfaces polished with 120 and 2400 grit paper and their respective replicas, calculated using high-pass and low-pass Gaussian filters, Robust filters and Spline filters.

A quicker comparison of the quality of replication of the different surfaces can be achieved by observing the values of the indicator Deft (table 1). The latter is the ratio of the number of F-values that are larger than one, divided by the total number of F-values. Thus, if Deft is equal to zero, then no significant differences are observed in the examined roughness parameters, whatever the scale and type of filter. Conversely, if Deft is larger than zero, it means that some differences are observed between the roughness parameters of the replica and the original surface; one or more roughness parameters have significantly different value at certain scales. It can be seen that the lowest value of Deft is obtained for the specimen polished with 120 grit paper, which means that the lowest differences between the roughness parameters of the original surface and its replica are observed.

Globally, it seems that, with the MD3P replica, there is a smaller loss of replication fidelity for rough surfaces than for smooth surfaces. A possible explanation of this trend is the stress caused by polymerization. The latter may prevent an accurate replication of features having small amplitude and spacing. To test this hypothesis, the waviness and maximum height of the specimens should be observed. The roughness

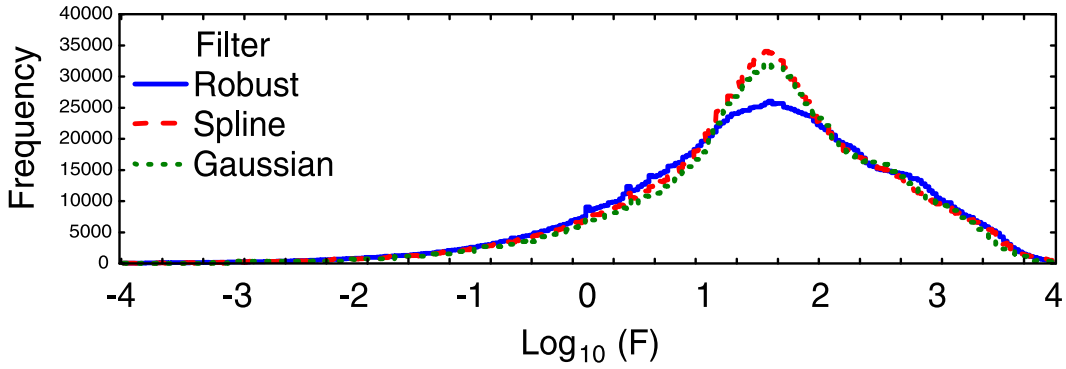

Figure A3. Histograms of the *F*-values for the Gaussian filter, Robust filter and Spline filter.

Table A1. Values of the statistics calculated using a Gaussian filter, a Robust filter and a Spline filter.

Statistics	Gaussian	Robust	Spline
F < 1 (%)	9.8	10.8	9.6
Mean	1.46	1.42	1.44
Standard deviation	1.08	1.10	1.16
P5	–0.60	–0.60	–0.58
P95	3.12	3.56	3.53

parameter enabling to analyze roughness maximum height is S_z while the one enabling to describe the surface global pattern is the autocorrelation length S_{al}. The latter represents the profile memory; it is the length from which the studied pattern will not be statistically defined. Figure 9 and figure 10 present, for the replica and the original surface, the autocorrelation length S_{al} and the maximum height of the surface S_z, respectively. It can be seen that the S_{al} parameter first decreases for grits ranging from 80 to 800 and then it increases for larger grit numbers. Conversely, the S_z parameter steadily decreases with an increase of the grit numbers. Thus, for specimens polished with coarse grit papers (e.g. Specimen 80), both the amplitude h and the length L over which it varies are large. Then, specimens polished with slightly finer grit papers show a decrease of both the amplitude and the variation length with certain proportionality of the ratio h/L (e.g. Specimen 220). Finally, for specimens polished with very fine grit papers (e.g. Specimen 2400), this proportionality between the amplitude and the variation length disappears; the amplitude keeps decreasing compared with surfaces obtained with coarser grit papers, while the variation length increases. This loss of proportionality occurs because the surface waviness can no longer be neglected compared to the surface roughness. These variations, summarized in figure 11, probably explain why rough surfaces are better replicated than smooth surfaces.

Physically, the resin undergoes volumetric shrinkage during polymerization. Indeed, as more and more monomers react, the developing polymer network becomes more rigid. The shrinkage of the system results in stress that can no longer be dissipated by the mobility of the monomers. This stress is trapped within the replica and exerts forces on the bonded interfaces. If a bonded surface is weaker than the shrinkage force, then it will de-bond from the surface and will cause a gap between the surface and the replica. When waviness is larger than roughness, the stress state probably tends to become unidirectional instead of bidirectional thus explaining the loss of replication accuracy.

5. Conclusion

Depending on the analysis goals, three main ways of assessing replication accuracy were identified: quantification of ‘metrological replication accuracy’, ‘physical replication accuracy’ and ‘functional replication accuracy’. Metrological replication accuracy was presented in this paper. It refers to the direct comparison of the roughness of the studied surface and its replica. A methodology enabling us to quantify metrological replication was presented. It uses an analysis of variance to rank the degree of resemblances of the original surface and its replica, over different scales. The *F*-mean is a good indicator for the assessment replication accuracy but does not enable us to quantify the differences between the replica and the original surface. The observation of the transfer function of the studied roughness parameters enables this quantification. Finally, the default indicator enables one

Table A2. Values of the indicator of defaults Deft for the replication of the specimens polished with paper grit 80, 120, 220, 500, 800, 1200 and 2400, calculated using a Gaussian filter, a Robust filter, a Spline filter and a Standard Gaussian filter.

Specimen	80	120	220	500	800	1200	2400
Gaussian	0.85	0.73	0.86	0.96	0.97	0.96	0.97
Robust	0.79	0.72	0.85	0.90	0.91	0.94	0.95
Spline	0.81	0.72	0.87	0.92	0.94	0.93	0.90
Standard Gaussian	0.82	0.75	0.87	0.91	0.94	0.94	0.94

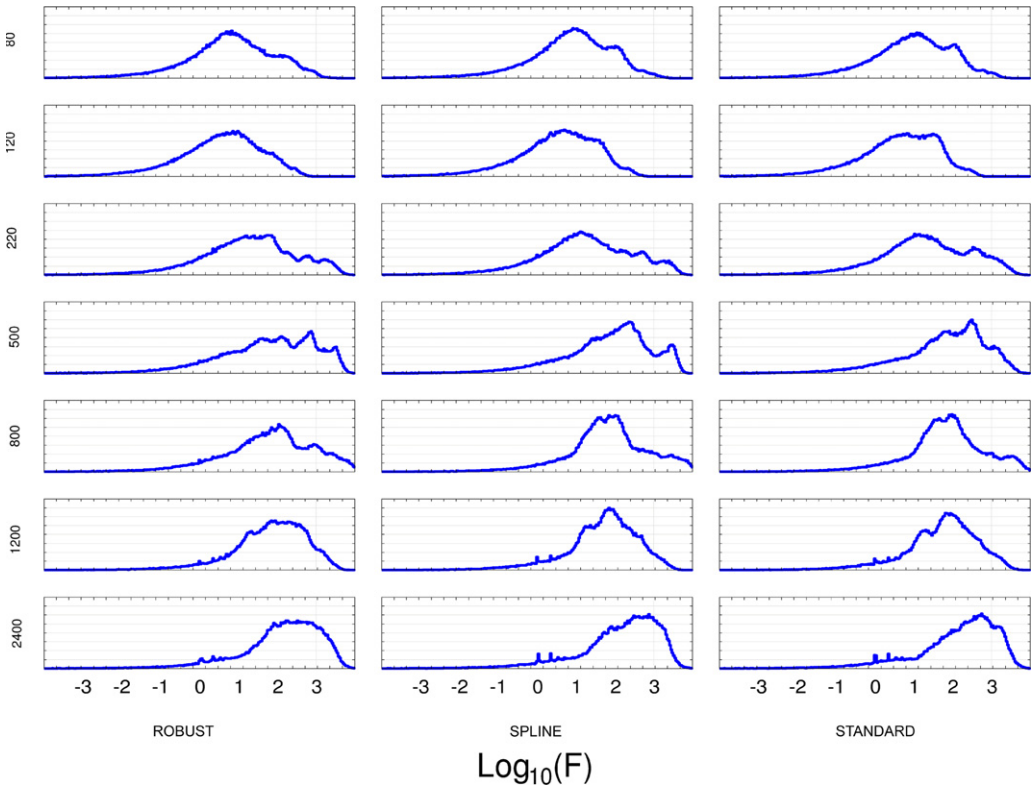

Figure A4. Histograms of the F-values for the Gaussian filter, Robust filter and Spline filter, for the specimens that were polished with 80, 120, 220, 500, 800, 1200 and 2400 grit paper.

to quickly compare the replication accuracy of a series of surfaces. The observations of these parameters enabled us to show that the tested replica material gives better results for rough surfaces than smooth surfaces.

The following studies will be focused on the quantification of physical and functional replication accuracy.

Appendix : Influence of the choice of filter on the results

To assess replication accuracy, a Gaussian filter was used. However, one question arises: Do the transfer function results depend on the choice of filter? To answer this question, the results of three different filters defined in roughness standards were compared. The filters are a Gaussian filter (Standard 16610-61), a Robust filter (16610-71) and a Spline filter (16610-62).

First, the values of different roughness parameters were calculated using these three filters, either using a high-pass or a low-pass. Figure A1 shows the results for the arithmetic mean deviation S_a, for the original surfaces polished with paper grit 120 and 2400 and their respective replicas. It can be seen that the value of S_a depends on the filter type for both types of specimens. Indeed, globally, the S_a values are subjected to the same trends. As an example, when using a low pass filter, S_a tends to decrease with an increase of the cut-off length for both specimens, whatever the type of filter that is used. But for the replica, the low-pass Robust filter gives lower S_a values than the low-pass Spline and Gaussian filters, which give similar values. Thus, the values of the calculated roughness parameters statistically differ for a given scale, due to the different filter responses. However, these values are not relevant for the assessment of replication accuracy. The relevant parameter is the 'difference' between the replication and the original. Figure A2 shows the results given by the transfer functions of S_a when using low-pass and high-pass Gaussian filters, Spline filters and Robust filters. Similar results are obtained for the transfer function, whatever the type of filter. Thus, the transfer function results do not depend on the filter type. It means that the three filters provide the same characterization for the calculation of the transfer function of S_a, for all paper grit numbers.

It is difficult to compare different types of filters. For this analysis, the best filter is the one that:

- Identifies scales where there is a lack of replication accuracy,
- Does not introduce bias i.e. it detects a difference that is not due to experimental conditions (border effects, sampling, …),
- Gives robust values for the transfer functions,
- Detects discrepancies of amplitude, as well as frequency, form and anisotropy.

Then, the meaning of 'quality of filtering' must be defined. First, the effect of the filter choice is assessed by taking into account all the roughness parameters and filtering conditions (DE, LP and HP), for all the scales and paper grits.

For the assessment of filtering quality, the same approach as the one used to test the difference between replication and original specimens is used (i.e. ANOVA method). For a given group of original and replication surfaces, the filter associated with a cut-off and type of filtering that gives the highest *F*-value for a roughness parameter will be considered as the best one because it enables to characterize the topographical difference using this parameter at this scale. In order to analyze all the *F*-values for the three examined filters, histograms and descriptive statistics are computed and shown in figure A3 and table A1.

According to table A1, the means and standard deviations are both similar. The 90% confidence intervals are also similar. It is worth noting that the number of values lower than 1 are the same whatever the examined filter (approximately equal to 10%). This means that good morphological replication does not depend on the filter type. Thus, on average, filters do not introduce artefacts preventing the good assessment of replication accuracy. However, it is important to note that having the same distribution does not imply that all the examined comparisons will have identical results. Indeed, a parameter associated with a filter may well distinguish the loss of replication accuracy for a given scale but results may vary with another filter. As a consequence, all filters defined by the standards have, on average, the same ability to characterize replication. Table A2 illustrates this point.

It is worth noting that, when analyzing the results by grit number, the shapes of the histograms are similar whatever the examined filter (as depicted by figure A4). On the contrary, their shape varies when the paper grit number changes. It means that the three filters enable us to quantify the studied transfer function with the same relevance.

References

[1] Xu C, Reece C and Kelley M 2013 Characterization of Nb SRF cavity materials by white light interferometry and replica techniques *Appl. Surf. Sci.* **274** 15–21

[2] Altıntaş E and Güngör E 2013 Alternative surface roughness measurement technique for inaccessible surfaces of jet engine parts using the rubber silicon replica method *Metallogr. Microstruct. Anal.* **2** 337–42

[3] Uemori N, Kakinoki Y, Karaki J and Kakigawa H 2012 New method for determining surface roughness of tongue *Gerodontology* **29** 90–5

[4] Masuda Y, Oguri M, Morinaga T and Hirao T 2014 Three-dimensional morphological characterization of the skin surface micro-topography using a skin replica and changes with age *Skin Res. Technol.* **20** 299–306

[5] Grove G L, Grove M J, Leyden J J, Lufrano L, Schwab B, Perry B H and Thorne E G 1991 Skin replica analysis of photodamaged skin after therapy with tretinoin emollient cream *J. Am. Acad. Dermatol.* **25** 231–7

[6] Le H R and Sutcliffe M P F 2000 Analysis of surface roughness of cold-rolled aluminium foil *Wear* **244** 71–8

[7] Yeo I W, de Freitas M H and Zimmerman R W 1998 Effect of shear displacement on the aperture and permeability of a rock fracture *Int. J. Rock Mech. Min. Sci.* **35** 1051–70

[8] Wieland M, Textor M, Chehroudi B and Brunette D M 2005 Synergistic interaction of topographic features in the production of bone-like nodules on Ti surfaces by rat osteoblasts *Biomater.* **26** 1119–30

[9] Gara L, Zou Q, Sangeorzan B P, Barber G C, McCormick H E and Mekari M H 2010 Wear measurement of the cylinder liner of a single cylinder diesel engine using a replication method *Wear* **268** 558–64

[10] Suputtamongkol K, Wonglamsam A, Eiampongpaiboon T, Malla S and Anusavice K J 2010 Surface roughness resulting from wear of lithia-disilicate-based posterior crowns *Wear* **269** 317–22

[11] Frazier W, Danks D R and Hodge B 2009 Paper pulp refiner long-duration wear monitoring with polymer replicas *Wear* **267** 1095–9

[12] Young A P and Schwartz C M 1960 A replica method for examining wear and scuffing in cylinder liners *Wear* **3** 235–40

[13] Newman J A, Willard S A, Smith S W and Piascik R S 2009 Replica-based crack inspection *Eng. Fract. Mech.* **76** 898–910

[14] Jordon J B, Bernard J D and Newman J C Jr 2012 Quantifying microstructurally small fatigue crack growth in an aluminum alloy using a silicon-rubber replica method *Int. J. Fatigue* **36** 206–10

[15] Kikuchi K, Aiba S, O′Goshi K-I, Yanai M, Takahashi M, Kasai H and Tagami H 2002 Demonstration of characteristic skin surface contours of extramammary Paget's disease and parapsoriasis en plaque by image analysis of negative impression replicas *J. Dermatol. Sci.* **30** 20–8

[16] Yin L, Morita A and Tsuji T 2001 Skin premature aging induced by tobacco smoking: the objective evidence of skin replica analysis *J. Dermatol. Sci.* **27** 26–31

[17] Liu Y and Li G 2012 A new method for producing 'lotus effect' on a biomimetic shark skin *J. Colloid Interface Sci.* **388** 235–42

[18] Schulte A J, Koch K, Spaeth M and Barthlott W 2009 Biomimetic replicas: transfer of complex architectures with different optical properties from plant surfaces onto technical materials *Acta Biomater.* **5** 1848–54

[19] Liu Y C, Ling C Y, Malcolm A A and Dong Z G 2011 Accuracy of replication for non-destructive surface finish measurement *Singapore Int. NDT Conf. & Exhib.* (Singapore: NDT) pp 1–12

[20] Nilsson L and Ohlsson R 2001 Accuracy of replica materials when measuring engineering surfaces *Int. J. Mach. Tools Manuf.* **41** 2139–45

[21] Balcon M, Marinello F, Tosello G, Carmignato S and Savio E 2011 Surface topography analysis for dimensional quality control of replication at the micrometre scale *J. Phys.: Conf. Ser.* **311** 012018

[22] Hansen H N, Hocken R J and Tosello G 2011 Replication of micro and nano surface geometries *CIRP Ann. Manuf. Technol.* **60** 695–714

[23] Stout K J, Matthia T, Sullivan P J, Dong W P, Mainsah E, Luo N and Zahouani H 1993 The developments of methods for the characterisation of roughness in three dimensions *Report EUR*

[24] ISO 25178-2 2012 *Geometrical Product Specifications (GPS) —Surface Texture: Areal—Part 2: Terms, definitions and surface texture parameters* (Geneva: International Organization for Standardization)

[25] ISO 13565-1 1996 *Geometrical Product Specifications (GPS) —Surface Texture: Profile method; Surfaces having stratified functional properties—Part 1: Filtering and general measurement conditions* (Geneva: International Organization for Standardization)

[26] ANSI/ASME B46.1 1996 *General description of profile parameters and fractal dimension*

[27] Ganti S and Bhushan B 1995 Generalized fractal analysis and its applications to engineering surfaces *Wear* **180** 17–34
[28] Bigerelle M, Najjar D and Iost A 2005 Multiscale functional analysis of wear: a fractal model of the grinding process *Wear* **258** 232–9
[29] Bigerelle M, Mathia T and Bouvier S 2012 The multi-scale roughness analyses and modeling of abrasion with the grit size effect on ground surfaces *Wear* **286–287** 124–35
[30] Hooge F N 1976 1/f noises *Physica A&C* **83** 14–23
[31] Gagnepain J J and Roques-Carmes C 1986 Fractal approach to two-dimensional and three-dimensional surface roughness *Wear* **109** 119–26
[32] Patrikar R M 2004 Modeling and simulation of surface roughness *Appl. Surf. Sci.* **228** 213–20
[33] Thomas T R, Rosén B G and Amini N 1999 Fractal characterisation of the anisotropy of rough surfaces *Wear* **232** 41–50
[34] Najjar D, Bigerelle M and Iost A 2003 The computer-based bootstrap method as a tool to select a relevant surface roughness parameter *Wear* **254** 450–60